

OligoHydrogelArray (OHA) for Parallelized Solid-Phase Extraction of Oligonucleotides

Michelle J. Iwohn, Maximilian Seifermann, Patrick Reiser, Julius Höpfner, Razan El Khaled El Faraj, Stefan Heißler, Anna A. Popova,* and Pavel A. Levkin*

Immobilization of oligonucleotides on solid surfaces is an important step in many experimental workflows in biology, such as gene expression analysis, genotyping, and drug discoveries. Capturing oligonucleotides in a highly efficient miniaturized format is still challenging. In this work, preparation of functionalized miniaturized acrylamide hydrogels on a droplet microarray (DMA) chip is reported. By further modification of these hydrogels through the Cu-catalyzed alkyne-azide cycloaddition, oligonucleotides are attached covalently, creating the OligoHydrogelArray (OHA). OHA enables the hybridization of oligonucleotides with defined sequences in a parallelized, miniaturized, and high-throughput manner with an overall loading capacity and extraction efficiency suitable for most biological and chemical applications. This system enables the parallelized solid-phase extraction of target oligonucleotides out of a mixture for purification and enrichment of DNA/RNA/PNA for application in fields such as transcriptomics. In the current study, we establish the chemical procedure for reproducible preparation of OHA and determine key characteristics, such as height, diameter, and shape of miniaturized gel pads as well as the loading capacity of oligonucleotides within the material. Finally, the ability to extract complementary oligonucleotide strands out of solution through hybridization is demonstrated to set the course for future applications.

medicine.^[1–3] Usually, readout methods to identify the effect of introduced stimuli on a cell, for example drugs, are based on analyzing phenotypic changes in the cells upon drug treatment. For this either microscopy-based methods are used, or a number of assays including viability and proliferation assays, reporter assays, biochemical assays such as kinase and protease assays, and others are performed.^[4] Changes at the molecular level, for example in mRNA transcripts by means of qPCR and mRNA sequencing, reflecting changes in gene expression upon drug treatment are very valuable and measuring these changes enables in-depth analysis of stimuli effect on the cells. However, the measurement of such molecular changes in high-throughput and especially miniaturized formats is challenging. Such methods usually require large amounts of starting material and include multiple steps of cell lysis, isolation, and purification of mRNA and its conversion to cDNA. Therefore, they are generally not compatible with throughput and miniaturization.


Platforms enabling high-throughput isolation of mRNA from cells in miniaturized format would enable the use of differential gene expression analysis as a read-out in high-throughput screening, which is not possible at the moment with existing workflows.

1. Introduction

Cell-based high-throughput screenings are essential in the fields of fundamental biology, drug discovery, and personalized

M. J. Iwohn, M. Seifermann, J. Höpfner, R. El Khaled El Faraj, A. A. Popova, P. A. Levkin
 Institute of Biological and Chemical Systems-Functional Molecular Systems
 Karlsruhe Institute of Technology
 Hermann-von-Helmholtz-Platz 1, 76344 Eggenstein-Leopoldshafen, Germany
 E-mail: anna.popova@kit.edu; levkin@kit.edu

P. Reiser
 Institute of Nanotechnology
 Karlsruhe Institute of Technology
 Hermann-von-Helmholtz-Platz 1, 76344 Eggenstein-Leopoldshafen, Germany
 S. Heißler
 Institute of Functional Interfaces
 Karlsruhe Institute of Technology
 Hermann-von-Helmholtz-Platz 1, 76344 Eggenstein-Leopoldshafen, Germany
 P. A. Levkin
 Institute of Organic Chemistry
 Karlsruhe Institute of Technology
 Fritz-Haber-Weg 6, 76131 Karlsruhe, Germany

 The ORCID identification number(s) for the author(s) of this article can be found under <https://doi.org/10.1002/admi.202300227>

© 2023 The Authors. Advanced Materials Interfaces published by Wiley-VCH GmbH. This is an open access article under the terms of the Creative Commons Attribution License, which permits use, distribution and reproduction in any medium, provided the original work is properly cited.

DOI: 10.1002/admi.202300227

In our group, we developed the “droplet microarray” (DMA) platform. It allows the formation of arrays of nanolitre (≈ 10 to 500 nL) droplets through hydrophilic spots separated by superhydrophobic borders on a microscope glass slide.^[5–9] Using the DMA platform, we have demonstrated various experimental applications such as cell-cell communication studies^[10] and drug screenings.^[11,12] The DMAs not only enable performing experiments in nanolitre volumes but also allow for the investigation of hundreds of different conditions in parallel on one slide. In order to enable analysis of differential gene expression after drug treatment in high-throughput, recently the methodology for extracting mRNA from live cells on DMA in a high-throughput manner, using OligodT magnetic beads was also demonstrated.^[13]

In order to simplify the purification of mRNA on the DMA chip and enable other types of applications with cell-derived RNA or DNA, we have suggested that this method would enable the binding of nucleic acid to the surface/hydrogel layer within each individual droplet directly on DMA after cell lysis. In the current study, we have introduced OligoHydrogelArray (OHA), where gel micropads polymerized in each hydrophilic spot of DMA are used for covalent immobilization of oligos, which can catch nucleic acids of defined sequences via hybridization for the subsequent analysis.

Attachment of DNA oligos for hybridization of the nucleic acids with defined sequences is used in multiple methodologies, including DNA microarrays, gene expression analysis, genotyping, quantitative protein profiling, antimicrobial drug discovery applications, DNA sensors, lab-on-chip platforms, flow cell for sequencing and microelectronic arrays.^[14,15] There are several approaches for surface modification used for attaching oligonucleotides to solid phases. Out of the many materials that have been tested such as nylon, silicon, Teflon, and gold, glass has proven to be the most useful one. It is cheap, has good chemical resistance, and can be easily modified by introducing required chemical groups on the surface.^[16] The glass substrate, however, provides only a 2D surface, which decreases its binding capacity.^[17] One possibility to increase the binding surface area of the glass substrate is to use controlled porous glass (CPG).^[18,19] Due to the voids, more molecules can be bound before leading to steric hindrance.^[20] Porous polymers^[21] and hydrogels^[22] are two materials that are also widely used for the covalent binding of oligonucleotides. They both provide a 3D network, which increases binding capacity by more than 100 times in case of polyacrylamide hydrogels in comparison to a 2D glass surface.^[23] For biological applications, hydrogels have advantages over porous polymers. Due to their loose network, hydrogels enable well-spaced immobilization of even large biomolecules, restricting their interference with each other.^[23,24] Additionally, hydrogels can be modified easily with different chemical groups^[25,26] and provide biocompatibility.^[27]

In the current study, we have utilized polyacrylamide hydrogels crosslinked with N,N'-methylenebis(acrylamide) (MBA) to form arrays containing 320 hydrogel pads of 1.5 μ L. Through the addition of acrylic comonomers bearing azide or disulfide groups, we introduced reactive groups, which could be used to attach modified oligos via copper(I)-catalyzed azide-alkyne cycloaddition or disulfide exchange, respectively. These reactions were chosen due to their high efficiencies under mild reaction conditions.^[28,29] The OHA platform can potentially be used as a

miniaturized high-throughput solid phase extraction (SPE) platform for the hybridization of DNA oligos of defined sequences within individual droplets. The ultimate goal of this methodology is to enable fast, one-step hybridization of nucleic acid with a defined sequence originating from cells treated by different stimuli for subsequent analysis.

2. Results and Discussion

2.1. Overview of OHA

A schematic depiction of the concept of fabrication of the OHA is shown in **Figure 1**.

As depicted, first 750 nL of an aqueous solution containing monomer, crosslinker, and tetramethylethylenediamine as catalyst for polymerization as well as 300 nL of a dimethyl sulfoxide (DMSO) solution containing comonomer are printed into each empty 320 hydrophilic spot (dimension 1400 μ m). As a second step, polymerization of the hydrogels is initiated through the addition of 450 nL of 37.7 mM ammonium persulfate aqueous solution. Superhydrophobic borders ensure the separation and stability of the individual hydrogel pads on the chip. Azide and disulfide groups are introduced through the N-(4-azidophenyl)acrylamide (6) and N-(2-pyridin-2-ylidysulfanyl)ethyl)acrylamide (9) comonomers (**Figure 2B**), which enable the covalent binding of oligonucleotides after polymerization via azide-alkyne cycloaddition or disulfide exchange, respectively. In the third step, the oligos for capturing are added and covalently bound through the hydrogel pads. Formed OHA is now able to capture nucleic acids from individual droplets.

2.2. Formation of Hydrogel Arrays

The properties of an OHA platform for capturing oligonucleotides are highly dependent on hydrogel composition. The hydrogels need to be stable on the DMA, insoluble in water, undetachable, should have the appropriate density to allow large biomolecules to diffuse into the network, and bear enough reactive groups with high enough reactivity to allow for a sufficient modification. These properties can be influenced by many parameters, in particular by monomers and crosslinkers used, crosslinking degree, and the ratio between co-monomers. In this section, we optimized the composition of hydrogels to provide optimal hydrogel properties.

For this study, we have used polyacrylamide hydrogels crosslinked with MBA (2), providing good biocompatibility, which is important for working with cells.^[30] The polymerization was carried out via thermally induced radical polymerization with ammonium persulfate (4) used as a radical initiator. Compared to UV-induced polymerization, the chosen method offers better compatibility with photodegradable reactive monomers. To functionalize the polymer network with reactive moieties for the covalent binding of oligonucleotides, reactive comonomers were added to the polymerization mixture (**Figure 2A**). Two different reactions were studied for the covalent binding of oligonucleotides. In the first one, 5'-alkyne-modified oligonucleotides (oligonucleotide 1) were used. Those were covalently attached to a hydrogel network via copper(I)-catalyzed azide-alkyne

Droplet Microarray
Platform

Parallelized Sequence Selective
Oligonucleotide Binding

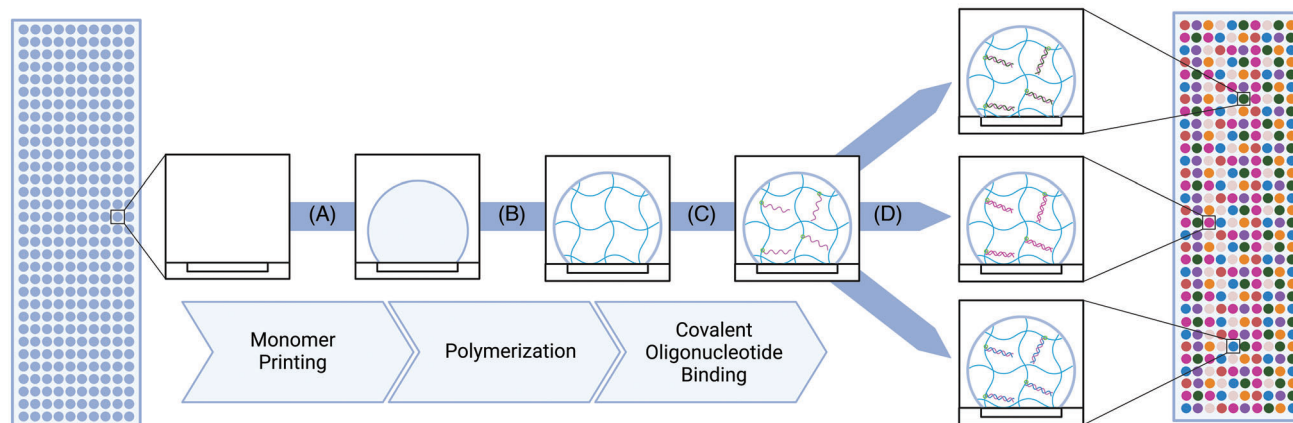


Figure 1. Schematic depiction showing the concept of OligoHydrogelArrays (OHA) for sequence selective oligonucleotide binding. The hydrophilic spots of the DMA act as a base for preparing an array of hydrogel pads. A) Solutions containing monomer and comonomers bearing azide or disulfide groups as well as tetramethylethylenediamine as polymerization catalyst were printed onto the hydrophilic spots. B) The polymerization was initiated by the addition of a solution containing ammonium persulfate. C) The reactive groups introduced through the comonomers allowed the covalent attachment of oligonucleotides via disulfide exchange or azide-alkyne cycloaddition post-polymerization. D) The hydrogel pads bearing oligonucleotides serve as a platform for many applications because parallelized sequence selective oligonucleotide binding via hybridization is enabled.

cycloaddition (CuAAC) between *N*-(4-azidophenyl)acrylamide (6) and an alkyne-modified oligonucleotide. In the second one, 5'-phosphorothioate-modified oligonucleotides were attached to hydrogels via disulfide exchange between *N*-(2-pyridin-2-yl)disulfanyl)ethyl)acrylamide (9) and a phosphorothioate-group of an oligonucleotide (oligonucleotide 3) (Figure 2B). Both methods have their advantages: CuAAC usually has a high reaction efficiency and the triazole-junction shows both high chemical and biochemical stability, whereas the disulfide bond is a reversible bond that allows for the reductive cleavage of oligos off the surface.^[31] This offers a toolbox to tailor the OHAs' properties to a variety of needs.

The modified oligonucleotides were commercially available, the acrylic comonomers were synthesized and added to the polymeric network in a ratio of 2 mol% (w.r.t. acrylamide). For the radical polymerization of the hydrogels, a thermal initiator system of ammonium persulfate (APS) (4) with tetramethylethylenediamine (TEMED) (3) as a polymerization catalyst was chosen. The presence of the reactive moieties in the hydrogels was proven by IR measurement (Figure 2C) for comonomer 6 and Raman measurement for comonomer 9 (Figure 2D).

2.3. Investigation of Gel Properties

In this part of the work, we have analyzed hydrogel properties that have a direct impact on their ability to bind oligonucleotides. We used acrylamide (1) as a monomer, which we copolymerized with two different acrylic comonomers *N*-(4-azidophenyl)acrylamide (6) and *N*-(2-pyridin-2-yl)disulfanyl)ethyl)acrylamide (9). Even though only 2 mol% (w.r.t. 1) of the comonomers were added to the polymerization mixture, they can impact the properties of the polymeric network due to their difference in size and hydrophilicity compared to unmodified acrylamide. The diffu-

sion rate, which describes the amount of material that can be intruded into the gel per time, decreases significantly with decreasing hydrophilicity of the monomers and increasing network density.^[32,33] Therefore, important properties of the two types of gels modified with comonomer 6 (gel3) or comonomer 9 (gel2) were investigated using different methods. The obtained properties were then compared to the properties of polyacrylamide gels without modification (gel1). Owing to the lower hydrophilicity of the moieties of comonomers 6 and 9 compared to acrylamide, it is possible that the network can be affected in its stability and swelling ratio. The swelling ratio refers to the ability of the hydrogel to swell in water. For the examination of the swelling ratio, the size of swollen and dried hydrogel pads, as well as the swelling ratio of bulk hydrogels, was investigated.

As a first step, we investigated the size of hydrogel pads after polymerization, as well as the swelling ratio of obtained hydrogels immediately after polymerization. We have compared three types of hydrogels: acrylamide (Equation (1)) crosslinked with methylenebis(acrylamide) (2) without addition of comonomer (gel1), with 2 mol% *N*-(2-pyridin-2-yl)disulfanyl)ethyl)acrylamide (9) (w.r.t. 1) (gel2) and with 2 mol% *N*-(4-azidophenyl) acrylamide (6) (w.r.t. 1) (gel3). The hydrogel pads were obtained by printing 1050 nL of pre-polymerization mixture per spot (spot dimension 1400 μm , distance between the spots 830 μm) on DMA, followed by the addition of 450 nL of a 37.7 mM aqueous ammonium persulfate solution to initiate radical polymerization. After polymerization for 90 min, the remaining liquid was taken off the gel pads by absorption with a lint-free tissue and side-view images were taken immediately (Figure 3A). To investigate the swelling rate of obtained hydrogel pads, the images of the same hydrogel pads were taken after swelling the gels in water for 24 h. The swollen hydrogels showed the same diameters and heights as directly after the polymerization, meaning that the gels reached their full swollen capacity already after the polymerization. The

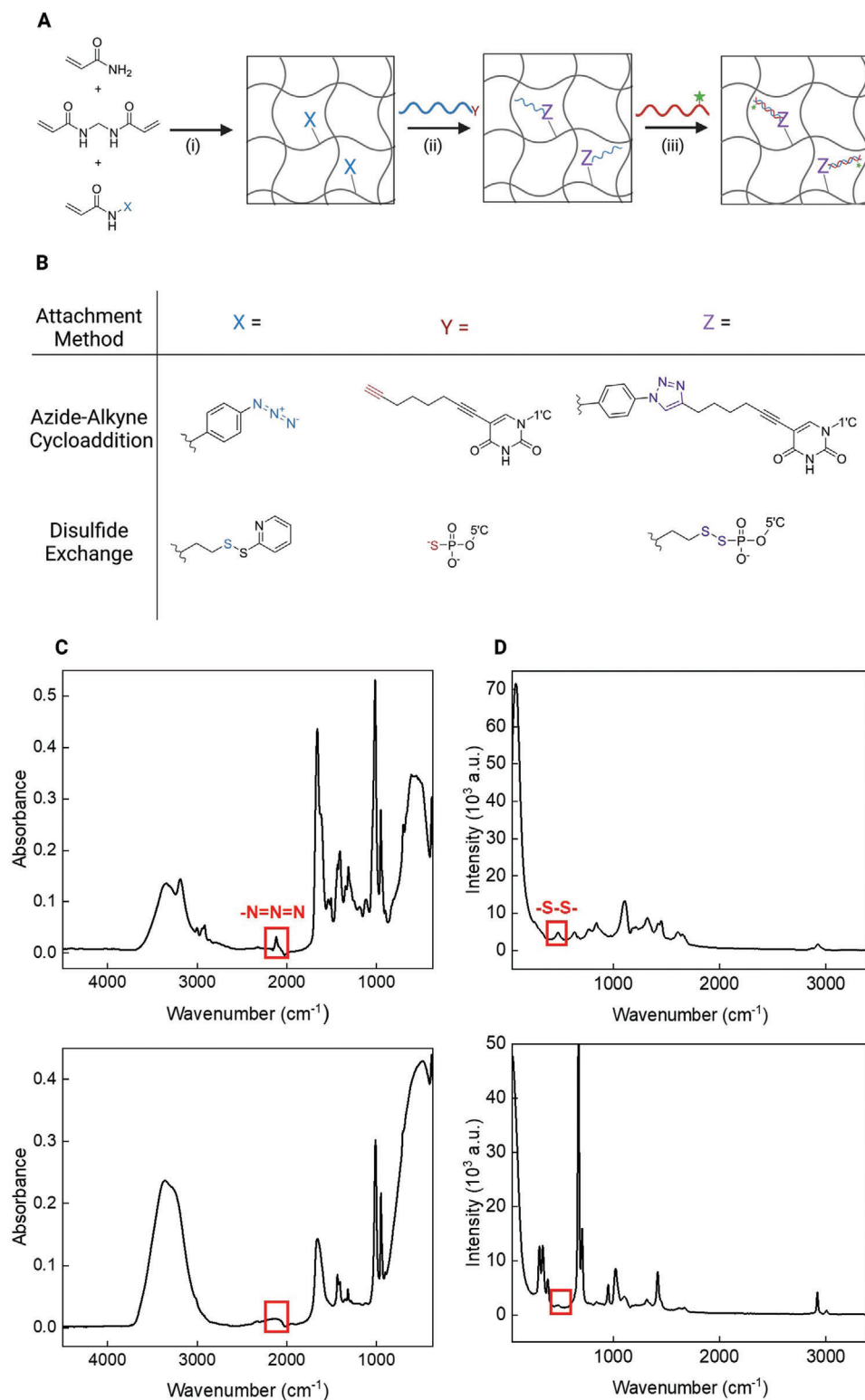


Figure 2. General workflow for the preparation and chemical characterization of the two different types of hydrogels. A) Experimental procedure consisting of three steps: i) Radical polymerization with ammonium persulfate (4) of different hydrogels with acrylamide (1) as a monomer and *N,N'*-methylenebis(acrylamide) (2) as a crosslinker. Hydrogels were supplemented with two different functionalized monomers 6 and 9 for subsequent steps. Functional groups for later binding of oligonucleotides are depicted as X. ii) Covalent binding of oligonucleotides to the reactive moieties of the hydrogels through disulfide exchange or azide-alkyne cycloaddition between the functionalized monomers and the functionalized oligonucleotides on 5'-end (Y) to yield the chemical junctions Z. iii) Hybridization of fluorescently labeled oligonucleotides that are complementary to the covalently bound oligonucleotides.

comparison between non-functionalized and two types of functionalized hydrogels showed that they had different sizes. Compared to the gels functionalized with 9, the gels functionalized with 6 were 16% and 27% smaller in height and diameter, respectively (Figure 3A). Therefore, the aryl-azide moiety affected the physical parameters of the gel to a greater extent compared to pyridyl disulfide. However, the influence of both comonomers on gel properties was visible when comparing their size to the size of gels without the supplementation of a comonomer. The diameters of both gel1 and gel2 are comparable to each other, but the heights of both functionalized gels were significantly smaller. The heights of gel2 and gel3 were 42% and 52% smaller compared to gel1. The measurements show that even low amounts of a less polar molecule can affect the size of the gel significantly.

As a next step, we measured the size of hydrogel pads after drying and their swelling rates. For this, the gels were polymerized on a DMA slide as described above with a total volume of 1.5 μL per spot. After polymerization, they were stained by swelling in rhodamine 6G solution, washed, and dried. Images of the hydrogels were taken with a fluorescence microscope (Figure 3B and 3C). The obtained images were analyzed to measure each individual pad's size as area exhibiting a color intensity above a certain threshold. Compared to the unmodified gel1, gel2 covered a much larger area and gel3 was considerably smaller (Figure 3D and Figure S12, Supporting Information). Especially the larger size of gel2 compared to gel1 is significant as the measurements of swollen gels (Figure 3A) indicated comparable diameters and even a smaller height for gel2 compared to gel1. The results from this measurement therefore indicate less shrinking of gel2 which was modified with acrylic disulfide upon drying.

The swelling rate of dried hydrogels is an important property that indicates the density of the network and therefore can be reflective of the ability of the hydrogel to incorporate molecules or even larger objects like cells. The swelling rate depends mainly on the abundance of hydrophilic groups in the network and on the crosslinking degree. Acrylamide used as the main monomer bears many hydrophilic groups, therefore all the gels exhibited a high swelling rate. The swelling rate of all three different gel types was measured by the weight difference between the swollen and dried state of gels polymerized from a 300 μL pre-polymerization mixture. The swelling rate of gel3 was the lowest and of gel2 the highest among the three types of obtained hydrogels (Figure 3E). However, the difference in swelling rates of all three hydrogel types was minimal (Figure 3E). As all three types can absorb around 2000% of water with respect to their dry weight, these slight differences should not have a great impact and the absorption capacity of all three hydrogel types for larger molecules is expected to be equal.

Taken together, we have established a protocol for the fabrication of OHA containing two types of functionalized hydrogels (gel2 and gel3) and have analyzed their size and swelling rates. The measurements showed a significant difference between the physical properties (size and swelling rates) of unfunctionalized polyacrylamide gels and the gels containing functionalized comonomers. However, both types of functionalized gels proved to build a stable network with a swelling rate sufficient for the planned application.

2.4. Covalent Binding of Oligonucleotides to Hydrogels

In this section, we have performed, optimized, and validated the binding of oligonucleotides to the hydrogel pads via azide-alkyne cycloaddition and disulfide exchange. We have used different reaction conditions to optimize the binding. To verify and compare the efficiencies of these two methods and the different conditions, we quantified the amount of oligonucleotides bound to gels by measuring the fluorescence intensity of labeled complementary oligonucleotides that were hybridized to the covalently bound oligos.

The covalent binding of oligonucleotides was based on two different types of reactions. In the first attachment method, the hydrogels with acrylic disulfide as a comonomer were used to perform a disulfide exchange. The reaction was carried out based on a published previously procedure.^[29] Therefore, the hydrogels were swollen in a potassium dihydrogen phosphate/potassium hydrogen phosphate buffer (pH = 7.4) before treating them with phosphorothioate-modified oligonucleotides dissolved in the same buffer. In contrast to the published procedure, the reaction was performed on a solid surface, which usually occurs significantly slower than a reaction in a solution.^[29] For this reason, the reaction time was increased to 21 h. In a second reaction type, the hydrogels with acrylic azide as a comonomer were used to perform an azide-alkyne cycloaddition. Again, the reaction was carried out in phosphate buffer for 21 h. In this reaction, the addition of DMSO as an auxiliary solvent together with copper(I) as a catalyst, a stabilizing ligand, and a reducing agent was necessary.^[34] The copper(I) ions were either added through copper(II)sulfate with sodium ascorbate as a reducing agent^[34–36] or through copper(I)bromide with ascorbic acid as a reducing agent.^[37] Tris(3-hydroxypropyltriazolylmethyl)amine (THPTA) was used as stabilizing ligand in both cases. For both methods of introducing the copper catalyst, the oligonucleotides were added in two different amounts. For each type of reaction, we have determined the amount of covalently bound oligonucleotides and their ability to hybridize their respective oligonucleotides. As every complementary strand is labeled with a fluorescence marker, the fluorescence of the gel increases with the amount of hybridized

cleotides. B) Detailed depiction of the chemical structures used for the covalent binding. X represents the residual groups used for the functionalization of acrylamide gels. Reactive units used for the first and second types of reactions are pyridyl disulfide or an aryl-azide, respectively. Y represents the modification of oligonucleotides. The modifications used for the first and second types of reaction were phosphorothioate bound to the 5'-carbon atom of the 5'-terminal deoxyribose and hepta-1,6-diyne-yl uracil bound to the 1'-carbon atom of the 5'-terminal deoxyribose, respectively. Z represents the junction obtained after the reaction between X and Y moieties took place, yielding either a disulfide or a triazole. C) IR measurements of a dried hydrogel functionalized with 10 mol% 6 (w.r.t. 1) (top) and without functionalization (bottom). The top graph shows the asymmetric N=N=N-stretch vibration at 2120 cm^{-1} , while the bottom graph shows no signal. D) Raman measurements of a dried hydrogel functionalized with 2 mol% 9 (w.r.t. 1) (top) and without functionalization (bottom). The top graph shows the S-S-band at 482 cm^{-1} , while the bottom graph does not show the signal in the area of interest.

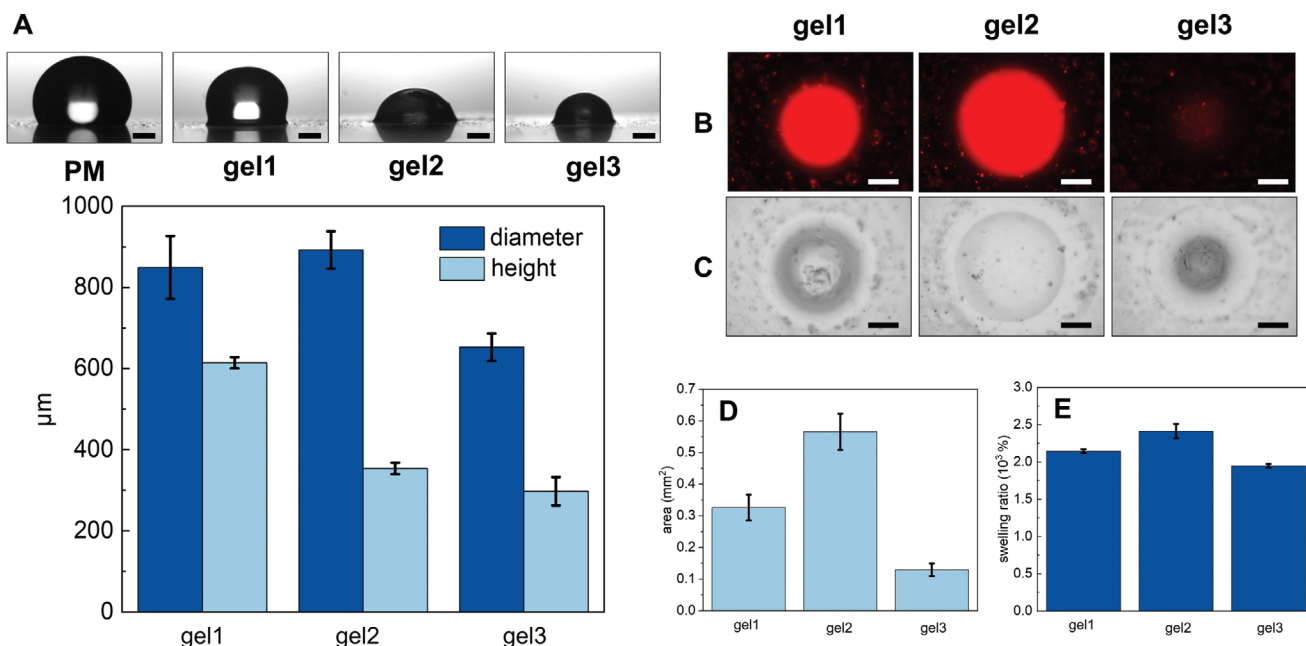


Figure 3. Characterization of three types of hydrogels: acrylamide (1) crosslinked with methylenebis(acrylamide) (2) without addition of comonomer (gel1), with 2 mol% *N*-(2-(pyridin-2-yl)disulfanyl)ethyl acrylamide (9) (w.r.t. 1) (gel2) and with 2 mol% *N*-(4-azidophenyl) acrylamide (6) (w.r.t. 1) (gel3). A) Representative side-view images of the pre-polymerization mixture (PM) and the three types of hydrogels (top) and each gel's respective width and height (bottom). Values were measured on 20 independent hydrogel pads for each type of hydrogel. The scale bars measure 150 μm. B) Representative microscope fluorescence images of rhodamine 6G stained and dried hydrogels (excitation time 5 ms). C) Representative microscope brightfield images corresponding to rhodamine 6G stained and dried hydrogels. The scale bars for (B,C) measure 250 μm. D) The area of rhodamine 6G stained and dried hydrogels. The measurements were done on 90 independent repetitions. E) Swelling rates measured from hydrogels polymerized with a total volume of 300 μL. Values were calculated from three independent repetitions. The microscope images used for the measurements were taken with a magnification factor of 10x and the hydrogels were polymerized with a total volume of 1.5 μL. All error bars represent standard deviations.

oligo strands to the covalently bound oligonucleotides in the gel. Thus, measuring the fluorescent intensity of the gels after the hybridization of oligonucleotides enables the estimation of the load of covalently bound oligonucleotides in the gels. The fluorescence intensity was evaluated by imaging the OHA with a fluorescence microscope and calculating the integrated pixel intensity of each gel. Hydrogels of the same composition without covalently bound oligos, but treated with the fluorescently labeled oligonucleotides served as negative controls (Figure 4A). To calculate the correlation between the fluorescence intensity of the gels and the number of bound oligonucleotides, calibration gels were made. For this, fixed amounts of fluorescence-labeled oligos were applied to hydrogels not following by washing of the OHA, and the fluorescence intensities of hydrogels containing different amounts of oligos were measured (Figure 4D,E). Using this method, we have demonstrated that the overall hybridizing capacity of the azide-alkyne cycloaddition is considerably higher than that of the disulfide exchange (Figure 4B,C). Furthermore, 35% more oligonucleotides were bound covalently when using copper(II)sulfate as a catalyst together with 1 pmol of oligonucleotides compared to copper(I)bromide under the same conditions. As expected, the amount of bound oligonucleotides in the gel is higher for the higher initial concentration (Figure 4B,C). Our results suggested that the best overall hybridizing capacity of hydrogels was obtained using azide-alkyne cycloaddition with copper(II)sulfate as a catalyst at an initial concentration of 1 pmol of the modified oligonucleotides. With this method, every

gel polymerized from the 1.5 μL polymerization mixture in OHA can hybridize around 131 fmol of oligonucleotides. As a typical mammalian cell contains around 60 attomoles of mRNA, each gel in OHA has the capacity to hybridize mRNA from 219 134 cells.^[38,39] For the potential cell-related applications on OHA this is more than enough, since up to a few hundred cells are usually cultured on each spot of DMA.

Thus in this section, we have created OHA using different reaction types and catalysts, and analyzed the hybridization capacity of all types of obtained hydrogels. We have shown that gels prepared using azide-alkyne cycloaddition with copper(II)sulfate as a catalyst, demonstrated the highest hybridization capacity, which in retrospect is sufficient for hybridizing mRNA from over 200 000 cells.

3. Conclusion

In this work, we developed a straightforward and affordable method for the preparation of cellcompatible hydrogel arrays (OHA) for sequence-selective solid-phase extraction of oligonucleotides. While the amount of non-covalent, and therefore non-selective oligonucleotides bound to the gel is comparably high (18% of specific binding), the selectivity of the sequence-selective binding is based on the selectivity of oligonucleotide hybridization. Therefore, the method has the same sequence selectivity as other such approaches. The fabrication process yields gels of homogeneous shape and size,

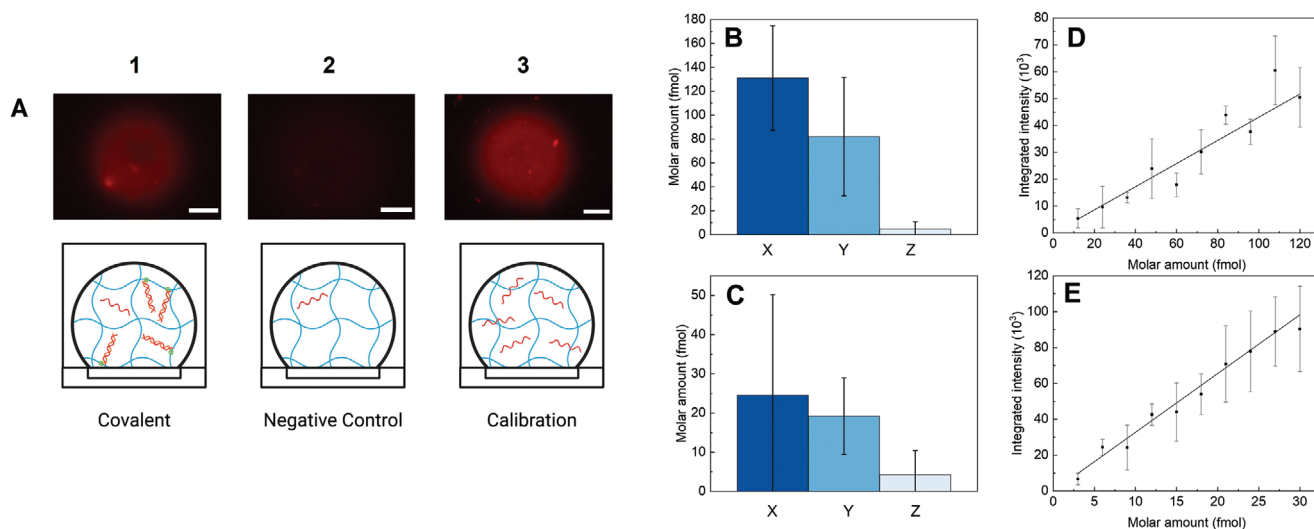


Figure 4. Quantification of the covalent binding of oligonucleotides to the two different hydrogels bearing a pyridyl disulfide or an aryl-azide as reactive unit treated with B) 1 pmol oligonucleotides or C) 0.2 pmol oligonucleotides. The charts show the number of oligonucleotides bound to hydrogels modified with 2 mol% *N*-(4-azidophenyl) acrylamide (6) (w.r.t. 1) or 2 mol% *N*-(2-pyridin-2-yl)disulfanyl)ethyl)acrylamide (9) (w.r.t. 1) via copper(I)-catalyzed azide-alkyne cycloaddition (X & Y) or via disulfide exchange (Z). Copper(II)sulfate (X) or copper(I)bromide (Y) were used as catalysts for the azide-alkyne cycloaddition with sodium ascorbate or ascorbic acid as reducing agents. The disulfide exchange was performed without the addition of a catalyst. The fluorescence-labeled complementary oligonucleotides were applied in an amount of 1 pmol. A1) Values were calculated from 15 to 16 independent repetitions by measuring the fluorescence area from the images of dried hydrogels with covalently bound oligonucleotides and fluorescence-labeled oligonucleotides after the removal of non-bound oligonucleotides. A2) To subtract the amount of non-chemically bound oligonucleotides in the gels, hydrogel pads containing the same comonomer were prepared and treated only with fluorescence-labeled oligos. A3) The correlation between the fluorescence intensity and the amount of covalently bound oligonucleotides was calculated by measuring the fluorescence intensity of 5 to 6 independent repetitions of dried hydrogels with 10 different amounts of C) fluorescence-labeled oligos complementary to the alkyne-modified oligonucleotides between 12 and 120 fmol or D) fluorescence-labeled oligos complementary to the phosphorothioate-modified oligonucleotides between 3 and 30 fmol. Error bars show the standard deviation. The scale bars measure 200 μ m. The excitation time for the representative fluorescence images was 100 ms.

indicating a reproducible procedure even under atmospheric conditions. With a maximum loading of 131 fmol per gel pad, the capacity of the gels is more than sufficient for a wide range of applications in the miniaturized format and theoretically enough to bind the mRNA of over 200 000 mammalian cells.

Our OHA approach allows the use of the array of hydrogel pads for parallel and miniaturized purification of specific oligonucleotide sequences out of the solution. It is designed to capture different types of oligonucleotides and can therefore be adapted to a specific application. Each of the 320 hydrogels can be designed to capture different types of oligos or capture oligos from different source liquids or from cells subjected to different stimuli. Therefore, OHA enables 320 parallel independent experiments on a single chip. OHA can be used as an improved platform for different types of experiments that require the purification of specific DNA or RNA strands. The reversible nature of oligonucleotide hybridization allows for a controlled release of nucleic acid after purification with a minimal loss of substance. Due to the biocompatibility of hydrogels used in our study, the OHA can be applied for cell assays where pure oligonucleotides (DNA or RNA) of a specific sequence are required for the readout, such as for example transcriptomics experiments. Since each separated hydrogel on the array can be modified independently, it is possible to either hybridize one type of oligos onto each hydrogel or different types of oligos for each hydrogel. In the first example, different stimuli could be introduced to cells on each pad to analyze the influence of different treatments on the abundance

of the same genes. In the second example, one could investigate different oligos in each hydrogel pad.

4. Experimental Section

Materials and Reagents: Modified oligonucleotides were purchased from Integrated DNA Technologies Germany GmbH. The sequence of the alkyne-modified oligonucleotides was 5'-/55OctdU/CA AGC AGA AGA CCG CAT ACG AGA T-3' (oligonucleotide 1). The sequence of the corresponding complementary strands was respectively 5'-/5TexRd-XN/ATC TCG TAT GCC GTC TTC TGC TTG-3' (oligonucleotide 2). The sequence of the phosphorothioate-modified oligonucleotides was 5'-T*TT TTT TTT TCA AGC AGA AGA CCG CAT ACGA-3' (oligonucleotide 3). The sequence of the corresponding complementary strands was respectively 5'-/5TexRd-XN/TCG TAT GCC GTC TTC TGC TTG AAA AAA AAA A-3' (oligonucleotide 4). 4-Azidoaniline hydrochloride, acryloyl chloride, hydrochloric acid, methanol, ethyl acetate, lithium chloride, acrylamide, *N,N'*-methylenebis(acrylamide), glucose, ammonium persulfate, copper(II)sulfate, tris(3-hydroxypropyl)triazolyl)methylamine, and silica gel were purchased from Sigma-Aldrich Chemie GmbH, Taufkirchen, Deutschland. Triethylamine, dry dichloromethane, and dimethyl sulfoxide were purchased from Fisher Scientific GmbH, Schwerte, Germany. Sodium hydrogen carbonate, sodium sulfate, acetic acid, diethyl ether, potassium dihydrogen phosphate, tetramethylethylenediamine, and tris-(hydroxymethyl)aminomethane hydrochloride were bought from Carl Roth GmbH + Co. KG, Karlsruhe, Germany. Chloroform, cyclohexane, trimethoxyvinylsilane, hydrochloric acid, and ethanol were purchased from VWR International, Radnor, PA, USA. 2-Mercaptoethylammonium chloride, 2,2-dipyridyl disulfide, potassium hydrogen carbonate, 2-mercaptoethanol, sodium ascorbate, and copper(I)bromide were bought

from Alfa Aesar GmbH & Co KG, Kandel, Germany. Glucose oxidase was bought from Amresco Inc., Solon, Ohio. AEROSIL 2000 was bought from Evonik Industries AG, Essen, Germany. 1H,1H,2H,2H-Perfluorodecanthiole was purchased from Genosynth GmbH, Berlin, Germany. Ascorbic acid was bought from Panreac Química SLU, Barcelona, Spain.

Measurements: NMR spectra of the synthesized molecules were measured with a Bruker Avance III HD 500 MHz at room temperature in deuterated solvents (chloroform, dimethyl sulfoxide) purchased from VWR International, Radnor, PA, USA. The peak shifts were declared in parts per million (ppm). The solvent peak served as a reference. For multiplets, the signal area was declared, for centrosymmetric signals, the center of the signal was declared. The description of the proton splitting occurred by using the abbreviations *s* for singlet, *d* for duplet, *t* for triplet, *q* for quartet, and *m* for multiplet. LCMS measurements were performed on an Agilent 1260 Infinity II system consisting of a quaternary pump (GB7111B;), autosampler (G7129A, 100 μ L sample loop), a temperature-controlled column oven (G7114A) and a variable UV-vis detector (G7114 A, VWD, flow cell G7114A 018, *d* = 10 mm, *V* = 14 μ L). Separation was performed on a C18 HPLC-column (Agilent Poroshell 120 EC-C18 4.6 \times 100 mm, 2.7 μ m) operating at 40 $^{\circ}$ C. A gradient of ACN:H₂O 10:90 – 80:20 *v/v* (additive 10 mmol L⁻¹ NH₄CH₃CO₂) at a flow rate of 1 mL \cdot min⁻¹ during 15 min was used as the eluting solvent. The flow was directed into an Agilent MSD (G6136BA, AP-ESI ion source). The instrument was calibrated in the *m/z* range 118–2121 in the positive mode and 113–2233 in the negative using a premixed calibration solution (Agilent). The following parameters were used: spray chamber flow: 12 L min⁻¹; drying gas temperature: 350 K, Capillary Voltage: 3000 V, Fragmentor Voltage: 100 V. Polymer samples for the measurement of IR and Raman spectra were prepared as described in “polymerization of hydrogels” with a total volume of 300 μ L and dried under vacuum. Polyacrylamide samples served as a reference. The IR spectra were measured with a Fourier transform infrared spectrometer Bruker Tensor 27 containing a Bruker platinum ATR unit with a diamond crystal. The measurement was performed in a range from 370 to 4000 cm⁻¹, at an angle of incidence of 45 $^{\circ}$ with a resolution of 4 cm⁻¹. The detector was an RT-DTGS and the software used was Bruker OPUS 8.5. The spectra were averaged over 32 single scans. The Raman spectra were measured with a Bruker Senterra 2.

Synthesis of *N*-(4-azidophenyl)acrylamide (6): A solution of 4-azidoaniline hydrochloride (5) (150.0 mg, 0.879 mmol, 1.0 Eq) and acryloyl chloride (78 μ L, 86.8 mg, 0.959 mmol, 1.1 Eq) in dry dichloromethane (10 mL) was cooled to 0 $^{\circ}$ C. Triethylamine (340 μ L, 250.0 mg, 2.47 mmol, 2.8 Eq) was added dropwise and the reaction was stirred for 1 h at 0 $^{\circ}$ C and for another 16 h at room temperature. The solution was evaporated to dryness, the residue was mixed with ethyl acetate (30 mL) and the suspension was filtered. The filtrate was washed with 10% hydrochloric acid (50 mL), saturated sodium bicarbonate solution (50 mL), and water (30 mL), dried over sodium sulfate and evaporated to dryness to afford the product as a yellow solid (112.0 mg, 0.595 mmol, 67%). ¹H NMR (500 MHz, DMSO-*d*₆, δ): 10.24 (s, 1H; NH), 7.74 – 7.70 (m, 2H; Ar H), 7.13 – 7.08 (m, 2H; Ar H), 6.42 (dd, *J* = 17.0, 10.1 Hz, 1H; CH), 6.26 (dd, *J* = 16.9, 2.0 Hz, 1H; CH₂), 5.77 (dd, *J* = 10.1, 2.0 Hz, 1H; CH₂); ¹³C NMR (126 MHz, DMSO-*d*₆, δ): 163.06 (C=O), 136.30 (C_q), 134.10 (C_q), 131.71 (CH), 127.02 (CH), 120.80 (CH₂), 119.52 (CH); LCMS *m/z*: [M+H]⁺ calc for C₉H₈N₄O, 189.077; found, 189.100.

Synthesis of 2-(pyridine-2-ylidysulfanyl)ethan-1-amine (8): According to the literature,^[40] a solution of 2-mercaptoethylammonium chloride (7) (129.4 mg, 1.14 mmol, 1.0 Eq) in methanol (1.13 mL) was added dropwise to a solution of 2,2-dipyridyl disulfide (500.0 mg, 2.27 mmol, 2.0 Eq) and acetic acid (83 μ L, 87.2 mg, 1.32 mmol, 1.2 Eq) in methanol (2.30 mL) over a period of 30 min. The reaction proceeded for 48 h at room temperature. The mixture was evaporated to dryness to afford a yellow oil which was washed with diethyl ether (10 mL) and dissolved in methanol (1.7 mL). The product was precipitated by adding diethyl ether (10 mL) and recovered by filtration. The precipitation process was repeated four times and the solid was dried under vacuum. The product was obtained as a white solid (212.2 mg, 1.14 mmol, 81%). ¹H NMR (500 MHz, D₂O, δ): 8.34 (dd, *J* = 5.2, 1.7 Hz, 1H; Ar H), 7.72 (td, *J* = 7.8, 1.8 Hz, 1H; Ar H), 7.63 (d, *J* =

8.1 Hz, 1H; Ar H), 7.22 (dd, *J* = 7.4, 5.0 Hz, 1H; Ar H), 3.24 (t, *J* = 6.3 Hz, 2H; CH₂), 3.00 (t, *J* = 6.3 Hz, 2H; CH₂); ¹³C NMR (126 MHz, D₂O, δ): 157.30 (C_q), 149.34 (CH), 138.59 (CH), 122.31 (CH), 121.85 (CH), 37.41 (CH₂), 34.76 (CH₂); LCMS *m/z*: [M+H]⁺ calc for C₇H₁₀N₂S₂, 187.036; found, 187.050.

Synthesis of *N*-(2-pyridin-2-ylidysulfanyl)ethylacrylamide (9): According to the literature,^[29] a solution of 8 (80.0 mg, 0.359 mmol, 1.0 Eq) and triethylamine (104 μ L, 75.9 mg, 0.750 mmol, 2.1 Eq) in chloroform (5 mL) was cooled to 0 $^{\circ}$ C. Acryloyl chloride (35 μ L, 39.0 mg, 0.431 mmol, 1.2 Eq) in chloroform (5 mL) was added dropwise over a period of 30 min. The reaction mixture was stirred overnight at room temperature and evaporated to dryness to afford a yellowish solid. The solid was mixed with ethyl acetate (8 mL), the suspension was filtered and the filtrate was evaporated to dryness. The product was purified by column chromatography [SiO₂, ethyl acetate – cyclohexane (1:1)] to afford the product as a yellowish oil (69.1 mg, 0.290 mmol, 80%). ¹H NMR (500 MHz, CDCl₃, δ): 8.52 (dd, *J* = 5.1, 1.8 Hz, 1H; Ar H), 7.64 (td, *J* = 7.7, 1.8 Hz, 1H; Ar H), 7.51 (d, *J* = 8.0 Hz, 1H; Ar H), 7.17 (dd, *J* = 7.4, 4.9 Hz, 1H; Ar H), 6.31 (dd, *J* = 17.1, 1.5 Hz, 1H; CH), 6.17 (dd, *J* = 17.1, 10.2 Hz, 1H; CH₂), 5.66 (dd, *J* = 10.2, 1.5 Hz, 1H; CH₂), 3.64 (q, *J* = 5.8 Hz, 2H; CH₂), 2.97 (dd, *J* = 6.6, 4.8 Hz, 2H; CH₂); ¹³C NMR (126 MHz, DMSO-*d*₆, δ): 165.21 (C = O), 159.49 (C_q), 150.10 (CH), 138.30 (CH), 131.97 (CH), 125.90 (CH₂), 121.70 (CH), 119.76 (CH), 38.27 (CH₂), 37.80 (CH₂); LCMS *m/z*: [M+H]⁺ calc for C₁₀H₁₂N₂OS₂, 241.047; found, 241.050.

Preparation of Buffer Solutions: A 100 mM K₂HPO₄/KH₂PO₄ buffer was prepared by dissolving 1.05 g potassium hydrogen phosphate and 1.91 g potassium dihydrogen phosphate in 200 mL deionized water. The pH value of this buffer was 7.43. A buffer consisting of tris(hydroxymethyl)aminoethane and lithium chloride was prepared by dissolving 8.48 g LiCl and 0.630 g tris in 200 mL deionized water. Therefore, the concentration of lithium chloride was 1 M and the concentration of tris(hydroxymethyl)aminoethane was 25 mM. The pH value of this buffer was 5.22.

Preparation of DMA Slides: The droplet microarrays were prepared according to a patented procedure.^[41] Uncoated Nexterion glass slides (Schott AG, Mainz, Germany) were activated by 10 min ozone treatment in an UVO-Cleaner (Jetlight Co. Inc., Irvine, CA, USA). Afterward, the slides were coated five times with 500 μ L of a solution containing AEROSIL 200 (Evonik Industries AG, Essen, Germany), trimethoxyvinylsilane (VWR, International, Radnor, PA, USA), and hydrochloric acid (VWR International, Radnor, PA, USA) in ethanol (VWR International, Radnor, PA, USA). The solution was spread evenly on the slide with a SPIN 150i spin coater (Polos by SPS, Putten, The Netherlands). After curing the slides for 1 h at 150 $^{\circ}$ C, they were washed with ethanol. To create the hydrophilic spots on superhydrophobic background, the slides were covered with a solution of 10 vol% 1H,1H,2H,2H-perfluorodecanethiole in isopropanol or 10 vol% mercaptoethanol in ethanol/water (1:1) and irradiated for 90 s using a UVA Cube 2000 (Dr. Hönl AG, Gilching, Germany).

Polymerization of Hydrogels: For preparing the hydrogels, four different solutions containing acrylamide (320 mg mL⁻¹), *N,N'*-methylenebis(acrylamide) (27.8 mg mL⁻¹), *N,N,N',N'*-tetramethylethylenediamine (52 μ L mL⁻¹), or glucose oxidase (7.8 mg mL⁻¹) were prepared with deionized water, degassed for 15 min in a sonicator, and mixed in equal ratios to afford solution 1. Solutions of glucose (8.4 mg mL⁻¹) and ammonium persulfate (8.6 mg mL⁻¹) were prepared with deionized water, degassed for 15 min in a sonicator, and mixed in equal ratios as well to afford solution 2. All these solutions were freshly prepared for every experiment. The comonomers were dissolved in dimethyl sulfoxide. The solutions of *N*-(4-azidophenyl)acrylamide (10.6 mg mL⁻¹) and *N*-(2-pyridin-2-ylidysulfanyl)ethylacrylamide (13.6 mg mL⁻¹) were stored at –20 $^{\circ}$ C between the experiments. For hydrogel pads on DMA, 300 nL of either a comonomer solution or dimethyl sulfoxide for gels without functionalization were printed first with a non-contact liquid dispenser (Cyger, Gwatt, Switzerland), then 750 nL of solution 1 and 450 nL of solution 2 were added. The total volume comprised 1.5 μ L. The ratios of the components in the final gels were 4 wt% acrylamide, 4 mol% methylenebis(acrylamide) (w.r.t. acrylamide), 1 mol% ammonium persulfate (w.r.t. acrylamide),

7.7 mol% tetramethylethylenediamine (w.r.t. acrylamide), and 2 mol% of the respective comonomer (w.r.t. acrylamide) for the functionalized gels. The concentrations of the degassing components were 6.1 μM glucose oxidase and 7.0 mM glucose. After printing, the slide was transferred to a "humidified Petri dish" which was prepared by layering the lid of a Petri dish (Corning, NY, USA) with a humidifying pad wetted with deionized water and adding 2 mL deionized water to the dish itself. The lid was closed and the Petri dish was allowed to stay at room temperature for at least 10 min. After transferring the slide to the prepared Petri dish, the lid was closed again and the gels were allowed to polymerize for 90 min at room temperature. Afterward, the slide was transferred to a falcon tube (Greiner Bio-One GmbH, Frickenhausen, Germany) containing 50 mL $\text{K}_2\text{HPO}_4/\text{KH}_2\text{PO}_4$ buffer and stored in the solution for at least 20 h either at room temperature or at 4 °C if the slide contained gels functionalized with *N*-(2-pyridin-2-ylidysulfanyl)ethyl)acrylamide.

Hydrogels in macroscale were polymerized in round spots of a PTFE mold with a total volume of 300 μL . The diameters of the spots comprised 1 mm. The ratios of the components were not changed. Therefore, 60 μL of either a comonomer solution or dimethyl sulfoxide, 150 μL of solution 1, and 90 μL of solution 2 were added to a spot of the mold and mixed. The gels were allowed to polymerize for 90 min at room temperature. Afterward, they were transferred to vials (VWR International, Radnor, PA, USA) containing 3.5 mL deionized water and stored in the solution for at least 20 h.

Covalent Binding of Oligonucleotides: Via Azide-Alkyne Cycloaddition: For the preparation of the catalyst solutions, dimethyl sulfoxide and $\text{K}_2\text{HPO}_4/\text{KH}_2\text{PO}_4$ buffer were degassed for 20 min with nitrogen. As a solvent, a 1:1 mixture of these liquids was used. The components were dissolved in the appropriate amount of $\text{K}_2\text{HPO}_4/\text{KH}_2\text{PO}_4$ buffer first before diluting the solution with dimethyl sulfoxide. The solutions contained 1.0 mg copper sulfate and 1.2 mg sodium ascorbate in 4 mL solvent (solution 3), 0.9 mg copper bromide and 1.1 mg ascorbic acid in 4 mL solvent (solution 4), 1.3 mg tris(3-hydroxypropyltriazolylmethyl)amine and 0.6 mg sodium ascorbate in 2 mL solvent (solution 5), and 1.3 mg tris(3-hydroxypropyltriazolylmethyl)amine and 0.6 mg ascorbic acid in 2 mL solvent (solution 6). All solutions contained the according components in a concentration of 0.5 mM. The solutions were prepared freshly for every experiment. Solutions 3 and 5 as well as solutions 4 and 6 were mixed in equal amounts directly before printing to yield solutions 7 and 8. The corresponding oligonucleotide solutions were prepared in two different concentrations. A 7.5 μM solution was prepared by mixing 1.5 μL of a 1 mM stock of oligonucleotide 1 with 200 μL of $\text{K}_2\text{HPO}_4/\text{KH}_2\text{PO}_4$ buffer, a 1.5 μM solution was prepared by mixing 1.5 μL of a 1 mM stock of oligonucleotide 1 with 1 mL of $\text{K}_2\text{HPO}_4/\text{KH}_2\text{PO}_4$ buffer. To ensure a complete transfer of the oligonucleotide stock solution, the pipette tip used for transferring the oligonucleotide stock solution was flushed several times with the diluted solution. The slide was removed from the buffer and overlapping liquid on the gels was allowed to dry for 10 min in a closed hood. 333 nL of either catalyst solution 7 or catalyst solution 8 and 167 nL of either the 7.5 μM or the 1.5 μM oligonucleotide solution were printed on every gel to yield a total volume of 500 nL on every gel. The total amounts of oligonucleotides therefore comprised either 1 or 0.2 pmol respectively. 500 nL of deionized water were printed on the gels functioning as negative controls. The slide was transferred to a humidified Petri dish, sealed with Parafilm (VWR International, Radnor, PA, USA), and incubated for 21 h at room temperature. Afterward, the slide was transferred to a falcon tube containing 50 mL of $\text{K}_2\text{HPO}_4/\text{KH}_2\text{PO}_4$ buffer and stored there for at least 30 h at room temperature.

Via Disulfide-Exchange: The corresponding phosphorothioate-modified oligonucleotide solutions were prepared in two different concentrations. A 2.5 μM oligonucleotide solution was prepared by mixing 1 μL of a 1 mM stock solution of oligonucleotide 3 with 400 μL $\text{K}_2\text{HPO}_4/\text{KH}_2\text{PO}_4$ buffer and a 0.5 μM oligonucleotide solution was prepared by mixing 0.5 μL of a 1 mM stock solution of oligonucleotide 3 with 1 mL $\text{K}_2\text{HPO}_4/\text{KH}_2\text{PO}_4$ buffer. To ensure a complete transfer of the oligonucleotide stock solution, the pipette tip used for transferring the solution was flushed several times with the diluted solution. The slide was removed from the buffer and overlapping liquid on the gels was allowed

to evaporate for 10 min in a closed hood. 500 nL of either the 2.5 μM or the 0.5 μM oligonucleotide solution was applied to each gel. The total amounts of oligonucleotides, therefore, comprised either 1 or 0.2 pmol. 500 nL of water were printed on the gels functioning as negative controls. The slide was transferred to a humidified Petri dish, sealed with Parafilm, and incubated for 21 h at room temperature. Afterward, the slide was transferred to a falcon tube containing 50 mL of $\text{K}_2\text{HPO}_4/\text{KH}_2\text{PO}_4$ buffer and stored there for at least 30 h at 4 °C.

Hybridization: To prepare the gels for hybridization, the slide was placed in a falcon tube containing 50 mL tris/LiCl buffer for at least 5 h. A 2 μM solution of the corresponding complementary strands was prepared by mixing 1 μL of a 1 mM stock solution of either oligonucleotide 2 for gels reacted via azide-alkyne cycloaddition or oligonucleotide 4 for gels reacted via disulfide exchange with 1 mL of tris/LiCl buffer. To ensure a complete transfer of the oligonucleotide stock solution, the pipette tip used for measuring was flushed several times with the diluted solution. The slide was removed from the buffer and overlapping liquid on the gels was allowed to evaporate for 10 min in a closed hood. 500 nL of the corresponding prepared complementary strand solution was printed on each gel. The amount of oligonucleotides printed on every gel, therefore, comprised 1 pmol. The slide was incubated in a humidified Petri dish sealed with Parafilm for 16 h at 37 °C. Afterward, the slide was transferred to a falcon tube containing 50 mL of $\text{K}_2\text{HPO}_4/\text{KH}_2\text{PO}_4$ buffer for at least 72 h.

Calibration Curve: Gels for calibration were printed on the same slide as the gels for covalent binding after hybridization and washing. Therefore, the slide was taken out of the buffer and the liquid on the empty spots used for printing the gels was allowed to evaporate for 5 min in a closed hood until dried. The gels were polymerized as described earlier. Afterward, the slide was transferred to a falcon tube containing 50 mL of deionized water and left there for at least 20 h. The slide was taken out of the water and the overlapping liquid on the gels was allowed to evaporate for 10 min in a closed hood. The calibration was performed by printing 50 to 500 nL of fluorescence-labeled oligonucleotide complementary strands on different gels in 50 nL steps. For the gels modified with *N*-(4-azidophenyl)acrylamide, a 0.24 μM stock solution of fluorescence-labeled complementary strands was prepared by mixing 240 μL of a 1 μM oligonucleotide stock solution with 760 μL of $\text{K}_2\text{HPO}_4/\text{KH}_2\text{PO}_4$ buffer. Therefore, the number of oligonucleotides added to each gel comprised 12 to 120 fmol in steps of 12 fmol. For the gels modified with *N*-(2-pyridin-2-ylidysulfanyl)ethyl)acrylamide, a 0.06 μM solution of fluorescence-labeled complementary strands was prepared by mixing 60 μL of a 1 μM oligonucleotide stock solution with 940 μL of $\text{K}_2\text{HPO}_4/\text{KH}_2\text{PO}_4$ buffer. Therefore, the number of oligonucleotides added to each gel comprised 3 to 30 fmol in steps of 3 fmol. To ensure a complete transfer of the oligonucleotide stock solution, the pipette tip used for transferring was flushed several times with the diluted solution in both cases. Negative controls were included where no oligonucleotide solution was printed on the gel. After printing, the slide was incubated in a humidified Petri dish at room temperature for 10 min. Afterward, the gels were dried in a closed hood for 3 h.

Evaluation: An image of the slide was taken with a fluorescence microscope with an excitation time of 1 s. The image was evaluated with an in-house developed software tool for automatic droplet grid- and edge-detections, featuring a graphical user interface for supervision and adjustment. The code is available at https://github.com/aimat-lab/microdroplet_segmentation. For edge detection, a Sobel filter with median and Gaussian blurring from scikit-image was chosen.^[42,43] After droplet segmentation with a two-label watershed algorithm within each array box on the Sobel elevation map,^[43–45] the pixel size (fluorescence area) and integrated gray-scale intensities (integrated intensity) of each droplet were recorded. To subtract the amount of non-chemically bound oligonucleotides in case of the covalent binding or the self-fluorescence of the gels in case of the calibration, the average of the integrated fluorescence intensities of the corresponding negative controls was calculated and subtracted from the integrated intensities of the other gels.

Calculation of the Swelling Rate: Hydrogels were polymerized on a macroscale as described earlier. After swelling, the gels were transferred to Petri dishes, weighed, dried at 80 °C, and weighed again. The swelling

rates were calculated with Equation (1).

$$\%SR = \frac{(Ws - Wd)}{Wd} * 100 \quad (1)$$

(SR = swelling rate, Ws = weight swollen, Wd = weight dried)

Supporting Information

Supporting Information is available from the Wiley Online Library or from the author.

Acknowledgements

M.J.I. and M.S. contributed equally to this work. This project was partly supported by DFG (Heisenbergprofessur Projektnummer: 406232485, LE 2936/9-1). Furthermore, the authors thank the Helmholtz Program "Materials Systems Engineering" for the support. The authors also thank Florian Feist (Institute of Nanotechnology, KIT) for help with the LCMS measurements.

Open access funding enabled and organized by Projekt DEAL.

Conflict of Interest

The authors declare no conflict of interest.

Data Availability Statement

The data that support the findings of this study are available from the corresponding author upon reasonable request.

Keywords

droplet microarrays, high-throughput, miniaturized hydrogels, oligonucleotides, parallelization, solid-phase extraction

Received: March 17, 2023

Revised: May 12, 2023

Published online:

- [1] M. Benz, A. Asperger, M. Hamester, A. Welle, S. Heissler, P. A. Levkin, *Nat. Commun.* **2020**, *11*, 5391.
- [2] F. Fanizza, M. Campanile, G. Forloni, C. Giordano, D. Albani, *J. Tissue Eng.* **2022**, *13*, 20417314221095339.
- [3] Y. Xia, H. Chen, J. Li, H. Hu, Q. Qian, R. X. He, Z. Ding, S. S. Guo, *ACS Appl. Mater. Interfaces* **2021**, *13*, 23489.
- [4] H. Aldewachi, R. N. Al-Zidan, M. T. Conner, M. M. Salman, *Bioengineering* **2021**, *8*, 30.
- [5] A. A. Popova, K. Demir, T. G. Hartanto, E. Schmitt, P. A. Levkin, *RSC Adv.* **2016**, *6*, 38263.
- [6] Y. Liu, S. Chakraborty, C. Direksilp, J. M. Scheiger, A. A. Popova, P. A. Levkin, *Mater. Today Bio* **2021**, *12*, 100153.
- [7] W. Feng, L. Li, E. Ueda, J. Li, S. Heißler, A. Welle, O. Trapp, P. A. Levkin, *Adv. Mater. Interfaces* **2014**, *1*, 1400269.
- [8] G. E. Jogia, T. Tronser, A. A. Popova, P. A. Levkin, *Microarrays* **2016**, *5*, 28.
- [9] T. Tronser, K. Demir, M. Reischl, M. Bastmeyer, P. A. Levkin, *Lab Chip* **2018**, *18*, 2257.
- [10] A. N. Efremov, E. Stanganello, A. Welle, S. Scholpp, P. A. Levkin, *Bio-materials* **2013**, *34*, 1757.
- [11] A. A. Popova, S. Dietrich, W. Huber, M. Reischl, R. Peravali, P. A. Levkin, *SLAS Technol.* **2021**, *26*, 274.
- [12] M. Benz, M. R. Molla, A. Böser, A. Rosenfeld, P. A. Levkin, *Nat. Commun.* **2019**, *10*, 2879.
- [13] S. Chakraborty, C. Luchena, J. J. Elton, M. P. Schilling, M. Reischl, M. Roux, P. A. Levkin, A. A. Popova, *Adv. Healthcare* **2022**, *11*, 2102493.
- [14] V. Grover, M. L. Pierce, P. Hoyt, F. Zhang, U. Melcher, *J. Virol. Methods* **2010**, *163*, 57.
- [15] A. Relógio, C. Schwager, A. Richter, W. Ansorge, J. Valcárcel, *Nucleic Acids Res.* **2002**, *30*, 51.
- [16] D. Sethi, R. P. Gandhi, P. Kuma, K. C. Gupta, *Biotechnol. J.* **2009**, *4*, 1513.
- [17] N. Zammattéo, L. Jeanmart, S. Hamels, S. Courtois, P. Louette, L. Hevesi, J. Remacle, *Anal. Biochem.* **2000**, *280*, 143.
- [18] S. S. Ghosh, G. F. Musso, *Nucleic Acids Res.* **1987**, *15*, 5353.
- [19] B. Joos, H. Kuster, R. Cone, *Anal. Biochem.* **1997**, *247*, 96.
- [20] S. Kralj, A. Zidanšek, G. Lahajnar, S. Žumer, R. Blinc, *Phys. Rev. E* **1998**, *57*, 3021.
- [21] B. C. Satterfield, S. Stern, M. R. Caplan, K. W. Hukari, J. A. A. West, *Anal. Chem.* **2007**, *79*, 6230.
- [22] J. Liu, *Soft Matter* **2011**, *7*, 6757.
- [23] D. Guschin, G. Yershov, A. Zaslavsky, A. Gemmel, V. Shick, D. Proudnikov, P. Arenkov, A. Mirzabekov, *Anal. Biochem.* **1997**, *250*, 203.
- [24] W. Zhan, H. N. Barnhill, K. Sivakumar, H. Tian, Q. Wang, *Tetrahedron Lett.* **2005**, *46*, 1691.
- [25] I. Kosif, E. J. Park, R. Sanyal, A. Sanyal, *Macromolecules* **2010**, *43*, 4140.
- [26] K. Yao, G. Gong, Z. Fu, Y. Wang, L. Zhang, G. Li, Y. Yang, *ACS Macro Lett.* **2020**, *9*, 1391.
- [27] S. Naahidi, M. Jafari, M. Logan, Y. Wang, Y. Yuan, H. Bae, B. Dixon, P. Chen, *Biotechnol. Adv.* **2017**, *35*, 530.
- [28] J. E. Hein, V. V. Fokin, *Chem. Soc. Rev.* **2010**, *39*, 1302.
- [29] Y. Sugawara, T. Tamaki, H. Ohashi, T. Yamaguchi, *Soft Matter* **2013**, *9*, 3331.
- [30] D. Saraydın, S. Ünver-Saraydın, E. Karadağ, E. Koptagel, O. Güven, *Nucl. Instrum. Methods Phys. Res., Sect. B* **2004**, *217*, 281.
- [31] M. Sela, F. H. White, C. B. Anfinsen, *Biochim. Biophys. Acta* **1959**, *31*, 417.
- [32] K. Engberg, C. W. Frank, *Biomed. Mater.* **2011**, *5*, 055006.
- [33] M. P. Mullarney, T. A. P. Seery, R. A. Weiss, *Polymer* **2006**, *11*, 3845.
- [34] J. Qiu, A. H. El-Sagheer, T. Brown, *Chem* **2013**, *49*, 6959.
- [35] S. V. Giofrè, M. Tiecco, A. Ferlazzo, R. Romeo, G. Ciancaleoni, R. Germani, D. Iannazzo, *Eur. J. Org. Chem.* **2021**, *34*, 4777.
- [36] M. Warminski, J. Kowalska, J. Jemielity, *Curr. Protoc. Nucleic Acid Chem.* **2020**, *82*, 112.
- [37] P. Sangtrirutnugul, P. Maisopa, L. Chaicharoenwimolkul, A. Sunsin, E. Somsook, V. Reutrakul, *J. Appl. Polym. Sci.* **2013**, *127*, 2757.
- [38] G. Brady, *Yeast* **2000**, *3*, 211.
- [39] D. A. Jackson, A. Pombo, F. Iborra, *FASEB J.* **2000**, *2*, 242.
- [40] Y. W. Ebright, Y. Chen, P. S. Pendergrast, R. H. Ebright, *Biochemistry* **1992**, *31*, 10664.
- [41] P. Levkin, M. Grunze, Z. Dhong, K. Demir, S. Widmaier, M. Brehm, A. Popova, (Karlsruhe Institute of Technology), EP3733277, **2019**.
- [42] G. Bradski, J. Dobb's, *Softw. Tools Prof. Program.* **2000**, *120*, 122.
- [43] S. van der Walt, J. L. Schönberger, J. Nunez-Iglesias, F. Boulogne, J. D. Warner, N. Yager, E. Gouillart, T. Yu, *PeerJ* **2014**, *2*, 453.
- [44] J. D. Hunter, *Comput. Sci. Eng.* **2007**, *9*, 90.
- [45] P. Neubert, P. Protzel, in *2014 22nd Int. Conf. on Pattern Recognition*, IEEE, Stockholm, Sweden **2014**, p. 996.